EFDA–JET–CP(12)06/01

F. Romanelli
on behalf of JET EFDA contributors

Overview of the JET Results with the ITER-like Wall

Overview of the JET Results with the ITER-like Wall

F. Romanelli
on behalf of JET EFDA contributors*

JET-EFDA, Culham Science Centre, OX14 3DB, Abingdon, UK

** See annex of F. Romanelli et al, "Overview of JET Results", (24th IAEA Fusion Energy Conference, San Diego, USA (2012)).*

Preprint of Paper to be submitted for publication in Proceedings of the
24th IAEA Fusion Energy Conference (FEC2012), San Diego, USA
8th October 2012 - 13th October 2012

ABSTRACT

Following the completion in May 2011 of the shutdown for the installation of the beryllium wall and the tungsten divertor, the first set of JET Campaigns have addressed the investigation of the retention properties and the development of operational scenarios with the new plasma facing materials. The large reduction of the carbon content (more than a factor ten) led to a much lower radiation during the burn-through phase of the plasma initiation with the consequence that breakdown failures are almost absent. Gas balance experiments have shown that fuel retention rates with the new wall are in line with the ITER needs. The re-establishment of high-confinement scenarios compatible with the new wall has required an optimization of the control of metallic impurity sources and heat loads. Stable type I ELMy H-mode regimes with $H_{98,y2}$ close to 1 and β_N~1.6 have been achieved in high triangularity plasmas. The ELM frequency is the main factor for the control of the metallic impurities accumulation. Pedestal temperatures tend to be lower with the new wall, leading to somewhat reduced confinement, but nitrogen seeding restores high pedestal temperatures and high confinement. Compared with the carbon wall, major disruptions with the new wall show a lower radiated power and a slower current quench. The higher heat loads on plasma-facing components due to lower radiation, made the routine use of massive gas injection for disruption mitigation essential.

1. INTRODUCTION

ITER has adopted beryllium as first wall and tungsten as divertor armour material, to reduce the tritium inventory an order of magnitude below that observed with carbon plasma-facing components (PFC) [1]. JET has been upgraded through a number of projects [2] in order to address the engineering, physics and technology aspects of plasma operation in this new all metal combination and to provide the basis for the effective exploitation of ITER. A complete replacement of the JET PFCs from carbon (JET-C) to the combination foreseen for ITER (JET-ILW) was completed during a major shutdown started in October 2009 (Fig.1).

The installation of the ILW with more than 3000 tile assemblies [3] has been executed almost entirely by remote handling. The replacement of the PFCs was complemented by enhancements in Real-Time systems for wall temperature monitoring and plasma control, the latter designed to ensure adequate protection of the new wall. The Neutral Beam Heating (NBI) was upgraded from 20MW/10s pulse to 30MW/20s pulse routine operation and a High Frequency Pellet Injection (HFPI) system for plasma fuelling and ELM control studies was installed. A suite of new diagnostics comprising a sophisticated camera arrangement to be used for real time control was also developed. Since plasma operation was re-established in August 2011 the JET programme has been devoted to the investigation of the retention properties of the ILW and to the study of ITER operational scenarios with the new wall.

In section 2 we give an overview of all major engineering and operational results obtained with the ILW and the implications for ITER operation. In section 3 the development of ITER relevant scenarios in the new all-metal environment is presented, along with confinement and edge pedestal physics results. Conclusions and perspectives are presented in section 4.

2. OPERATION OF JET WITH THE ITER-LIKE WALL.

2.1 PLASMA IMPURITY CONTENT AND IMPURITY SOURCES FROM PLASMA FACING COMPONENTS

From the very first JET-ILW plasmas the impurity content has been significantly reduced as compared to JET-C conditions. The carbon content is on average a factor 20 lower than in comparable JET-C plasmas as taken by the density normalised intensity of CIII (97.7nm) line (Fig.2). There is no evidence of any significant increase in residual carbon in time, indicating that no damage of the W-coatings on CFC substrate in the divertor has occurred. Oxygen levels are also lower by roughly one order of magnitude with respect to JET-C with non-optimal wall conditions (although only marginally lower than in JET C-wall plasmas with well conditioned wall and following Be evaporations). This large reduction of residual impurity levels is similar to that found earlier by AUG when going from a all-C to a boronised [4] all-W wall. The line averaged Z_{eff} decreases from ~2 (JET-C) to 1.2 (JET-ILW) for similar values of density and heating power. The lower residual carbon and oxygen level in JET-ILW is thought to be mainly due to gettering of carbon and oxygen by beryllium [5].

Specific effort has been devoted to investigate the impact to the operational space due to W core accumulation [6] and surface melting [7]. Beryllium erosion can shorten component lifetimes, contribute to tritium retention by re-deposition [8] and cause significant sputtering of tungsten. Tungsten sputtering has been studied in L- and H-mode discharges. It is found that for the present range of temperatures and impurity content at JET most of the W sputtering in L-mode can be attributed to low Z impurities, more specifically Be ions (Fig.3**)**. Experiments in L-mode have been performed to compare the impurity content under neutral beam (NBI) and Ion Cyclotron Resoance Frequency (ICRF) heating. As shown in Fig.4, the bulk radiation, defined as power radiated from inside the separatrix, is higher with ICRF [9] although significant electron heating is obtained and the increase in plasma energy is similar to C-wall values. It was estimated that around 80% of the radiation comes from W and 20% by Nickel with sources from the divertor entrance and main chamber [10] [11]. The cause for this increased radiation remains the subject of ongoing investigation [9]. It could be due to the generation of fast Be ions in front of the antenna following the field lines to the divertor and giving rise to enhanced W sputtering. In H-mode plasmas, measurements of intra and inter ELM radiation from WI lines [12] indicate that ELM events dominate the sputtering of W (Fig.5).

Transient increases have been observed in total radiated power, probably associated with small particles of medium/high Z materials, mostly W, entering the plasma. Since the start of plasma operation with the ILW, the frequency of such events has first increased, with the progressive increase of the additional heating power to the plasma, and then decreased. These sudden influxes are not necessarily fatal for the plasma which often recovers from the increased radiation [13].

2.2. PLASMA BREAKDOWN AND CURRENT RUMP-UP

The strong decrease of carbon content in the machine with the ILW has lead to a significant reduction

of radiation during the burn-through phase of the plasma initiation. In Fig. 6 [14], the radiated power as a function of line-integrated density at the end of the burn-through phase is shown for JET-ILW and JET-C data.

In contrast to JET-C, a 1MA/15s plasma discharge was easily obtained at the first attempt during the restart. No failed breakdowns (e.m.f. in the range of 0.27 – 1.6 V/m) attributable to conditioning issues have been observed so far with the ILW. Furthermore, the JET-ILW experience shows no need for glow discharge cleaning or beryllium evaporation to improve wall conditions and facilitate plasma initiation.

Breakdown conditions have been studied and optimised in dedicated experiments. The on-axis electric field parameter space has been thoroughly explored and non-assisted breakdown has been routinely demonstrated down to the values expected in ITER (<0.35V/m) [14].

The measured duration of the avalanche phase is found to follow the scaling for a Townsend avalanche process. This phase of the breakdown process is dominated by the pre-fill gas and details of the error fields in the vessel, and not affected by the plasma-facing material. As expected, with decreasing electric field the avalanche phase was found to be more and more sensitive to the error field dynamics, eddy currents in passive structures and the behaviour of vertical stability control. The plasma-facing material had however a strong impact on the burn-through phase of the breakdown. Lower radiation at higher electron densities was achieved, making the breakdown more robust. Although common with the C-wall, no breakdown failures due to de-conditioning events, such as disruptions, happened with the ILWl [14][15]. A model of plasma burn-through has been developed integrating the break-down, plasma burn-through phase, the ramp-up of plasma current up to the flat-top and for the first time plasma-surface interaction effects [16] and has shown good agreement with the experimental results.

The impact of the ILW on the plasma current (I_P) diffusion during the I_P rise was studied in a series of experiments [17]. Plasmas with early X-point formation showed that during current ramp-up the temperature profile becomes hollow in the centre and lasts until the flat top phase. As a consequence the plasma develops a negative magnetic shear profile in contrast with similar shots in the JET-C, but without hollow temperature profile. In shots with increased electron density and higher central temperature a higher plasma inductance (l_i) is obtained as a result of increasing n_e during the limiter phase, indicating that the I_P profile at that time becomes relatively more peaked. A lower l_i (matching that of JET-C plasmas) can be recovered at the end of the I_P rise by adjusting n_e. Adding ICRH (1MW) resulted in a peaked Te profile. These shots showed weak positive shear by the time of the I_P flattop, indicating that the required q-profiles for hybrid and advanced scenarios on JET-ILW can be recovered.

2.3 FUEL RETENTION

One of the crucial operational and safety requirements for ITER is to keep the in-vessel tritium inventory within the safety limits [18]. This requirement led to the choice of a Be wall and a W divertor on ITER. In order to achieve this, the corresponding retention rate in JET D plasmas should

be below ~ 10^{20}D/s. The retention of D with the ILW has been investigated in JET via controlled experiments for several main plasma scenarios and compared with the retention in reference JET-C discharges. The vessel pumping was ensured purely by the cryopumps in the divertor region (in L-mode and type III ELMy H-Modes) and gas balance was estimated using vacuum gauges and D released during cryopumps regenerations. In addition, in order to have an independent determination of the fuel retention, an experiment based on repeated (~150) identical H-mode discharges (NBI: 11MW/6s), equalling roughly the divertor fluence of one ITER pulse, was performed at the end of the campaign followed by the removal of some ILW tiles for surface analysis. The D retention as a function of discharge type is presented in Fig.7 [19]. In comparison to JET-C the reduction in D retention in JET-ILW (1.4×10^{20} D/s for H-mode type-I) is at least tenfold, matching well the predictions [8].

The retention of D in the ILW is most likely due to co-deposition in Be layers. This seems to agree with the relatively high Be influx measured at the divertor inner leg where the D co-deposition is expected to be higher. For the JET characteristic exposure times (≈ 10s), JET-ILW shows a very reproducible dynamic fuel retention which is about 2-2.5 larger than JET-C with a negligible memory effect from previous plasma loading conditions [20]. Typical shot end retention is $1.5\text{-}3 \times 10^{22}$ D with short term excursions above 10^{23} D. This dynamic retention is sufficient to provide wall pumping in the start up phase of ITER.

2.4 DENSITY LIMIT AND DETACHMENT

Tokamak operation at high density with detached divertor is a key element of the current ITER baseline design. Detached divertor operation is mandatory to reduce the heat loads on the divertor target plates down to an acceptable level.

L-mode density limit experiments with the ILW have been performed at comparable plasma parameters of a wide set of reference JET-C reference, at BT=2.0T, Ip=2.0MA and ranging from purely ohmic to NBI heated conditions in both low- and high-triangularity magnetic configurations. The change in the main radiating species and the overall reduction in total radiation in JET-ILW has raised the L-mode disruptive density limit [21][22] by up to 30-40% in all magnetic configurations, including the ITER relevant vertical target configuration (Fig.8). In addition, significantly higher gas dosing rates (>10^{22} D/s) are needed to reach such limit in the JET-ILW then with the C wall.

The ILW has a substantial effect on the electron density and temperature at both strike points as well as on the detachment onset. In the JET-ILW, detachment in the inner and outer divertor legs occurs nearly simultaneously indicating a much smaller in-out divertor asymmetry. With strike points on the vertical divertor targets, the lifetime of the X-point MARFE is much longer for JET-ILW (200 ms) than for JET-C, giving the opportunity for testing feedback control schemes for stable fully-detached divertor operation.

2.5 DISRUPTIONS

The fraction of available magnetic and thermal energy radiated during disruptions has dropped

from 50-100% for JET-C down to 10% -50% for JET-ILW. The reduced radiation has important consequences for the timescales of the disruption process and its impact on PFCs. Higher plasma temperatures after the thermal quench, up to 1 keV, are observed in JET-ILW with a current decay time significantly longer than in JET-C. With the carbon wall, about 80% of all unmitigated disruptions had a linear normalised current quench time below 6ms/m^2. With the JET-ILW only 15% are in that range and 20% have a very long current quench well above 20ms/m^2. Due to the slow current quench higher halo fractions (up to 40%) are more likely to occur [15]. In JET-C the reaction of the vessel was found to scale proportionally to the halo current [23]. The reaction force or vessel displacement was found to vary with the magnitude of the force due to the halo current, as shown in Fig. 9, but also with the impulse (i.e. the time integrated force). Hence, the longer current quench duration also led to larger impulses and thus larger reaction forces on the vessel.

Because of the lower radiation a larger fraction of the energy is conducted to the PFCs for unmitigated ILW disruptions. Temperatures close to Be melting point (1278 °C) have been measured by IR cameras, with some local melting being detected by subsequent visual inspection.

In order to mitigate the higher forces and heat loads, the use of real-time Massive Gas Injection (MGI) became essential to the operation of JET. MGI been fully integrated in most of the plasma scenarios that have the potential to generate high heat loads or forces. The use of MGI [24] has been extremely successful in mitigating disruptions in high-current H-modes up to 3.5 MA.

2.6 PLASMA FACING COMPONENTS POWER HANDLING AND PROTECTION

The design of the ILW components has taken into account plasma operation at high power (NBI 35MW and ICRF 5 MW) and high plasma current (disruptions up to 6MA). For example, due to constraints on the size of the tiles because of eddy currents and thermal and electromechanical stresses a completely new design was required. The Be tiles are made up of slices mounted in an Inconel rack with a castellated plasma-facing surface [25]. In addition, the tile profiles were optimised to maximise the power handling and no leading edges above 40 μm effective height are exposed in high heat flux areas [26]. This experience is of high relevance to the ITER PFCs design.

The thermal properties of the new wall materials results in new limits for heat loads to PFCs. The Be tiles are at risk of melting, rather than evaporating as CFC tiles, at lower wall temperatures (1278°C). In the divertor, the main risk for bulk W components is re-crystallization while for the W-coated CFC tiles the main limit is posed by carbidisation and inter-layer embrittlement. Thus, the limit for the surface temperature of the divertor components during the initial ILW campaigns was set between 1000 - 1200°C. An integrated protection of the ITER-like wall (PIW) was implemented. It comprises of CCD cameras, operating in the near infra-red and covering up to 66% of the PFCs and 43% of the divertor, linked to a Real-Time system connecting all main tokamak controls and heating systems [27]. Detection of high temperatures in one or more of the monitored regions triggers a tailored response, ranging from decreasing additional heating power, to changing the magnetic configuration and, in extreme cases, to the orderly termination of the plasma pulse. In the area covered by the CCD cameras no melt damage to the main JET limiters and no unexpected hot

spots on the inner and outer wall limiter surfaces have been observed. A single small melt spot on a limiter (Be) was caused by a runaway electron beam created during an emergency stop at the start of the campaign when the protection system was being commissioned. Limiters have been damaged in hidden areas from the protection cameras most due to identification of a toroidal asymmetry in the heat loads to the limiters.

Dedicated experiments have been carried out to verify the power handling limits set by the bulk W divertor with its lamella structure [28] and geometry. The bulk W divertor was designed to withstand loads up to 9MW/m^2 for a total conducted energy of 60MJ/m^2 and a maximum surface temperature of 2200^{o}C. Plasma operation with conducted energies of ~30MJ/m^2 has been performed routinely keeping the tile surface temperature below 1000^{o}C and the supporting structure below 360^{o}C. Conducted energies up to ~48MJ/m^2 have also been applied where the surface temperature reached ~1200^{o}C. Overall the bulk W tile has achieved the technical design requirements and no damage has been observed.

3. H-MODE PHYSICS IN ALL-METAL ENVIRONMENT

The qualification of the ELMy H-mode and of the hybrid regime with the ILW has provided a number of results of direct relevance for ITER.

3.1 L-H POWER THRESHOLD

A set of reference JET-C discharges was selected and closely matching JET-ILW discharges have been produced. In the reference JET-C discharges the L-H power threshold, P_{thr}, was found to be consistent with the multi machine ITPA scaling law [29] down to very low densities of $1x10^{19}$ m^{-3} [30], where previous JET-C experiments with the MkII-GB septum divertor had shown deviations from the scaling [31]. For JET-ILW the L-H power threshold is found to differ both in magnitude and in its dependence on the plasma density compared to the reference JET-C discharges, as shown in Fig.10 [32]. P_{thr} is reduced by ~ 30% at higher densities (>$2x10^{19}$ m^{-3}), while it increases below a minimum density (~$2x10^{19}$ m^{-3}) thus recovering the low density behaviour first observed with the earlier MkII-GB septum divertor in JET-C.

These findings apply both to Pthr and to the net power crossing the separatrix (namely, after subtraction of the core radiation the ICRH values practically overlap the NBI values). In addition, the minimum density ne,min and the minimum H-mode access power are found to increase roughly linearly with magnetic field.

A similar reduction in P_{thr} by ~ 25% has also been reported by AUG with W wall [33]. The L-H power threshold in JET-ILW is also sensitive to variations in divertor configuration and main plasma shape [32], features which are not captured in the ITPA scaling law. Comparison of the JET C and ILW dataset with a recently proposed local model for the L-H transition [34] is in progress.

3.2 BASELINE H-MODE SCENARIO

The baseline type I ELMy H-mode regime was re-established with the ILW as soon as NBI power

became available. As mentioned in section 2.1, the early H-mode experiments were affected by metallic impurity influx events, whose occurrence strongly decreased with further operation, suggesting a conditioning effect of the divertor surface.

By the end of the 2012 JET campaign, the operating space for baseline H-modes had almost recovered the full range of parameters explored with the C wall. H-mode discharges have been produced in both low and high triangularity (δ) configurations, mostly with the Inner Strike Point (ISP) on a W-coated vertical target and the Outer strike Point (OSP) on the bulk W tiles. A limited exploration of an ITER-relevant vertical target divertor configuration was, also, carried out. H-modes were produced with total injected power of 25.5MW up to 3.5MA at low δ (Pulse No: 83479). A representative H-mode shot with H_{98}~0.9 is shown in Fig.11 [35].

As already observed in AUG with the W wall [33], the behaviour of the baseline H-mode was influenced by the change of first wall and divertor materials. In type I ELMy H-modes at relatively low ELM frequency ~10-15Hz, e.g. at low power or low levels of gas dosing, typically < 10^{22} el/s at 2.5MA, the global confinement can transiently achieve H_{98}~1 but the discharge evolution tends to be dominated by W accumulation (Fig.12). W accumulation can be avoided and more stationary conditions can be obtained in H-modes at higher ELM frequencies, using significant amounts (> 10^{22} el/s) of gas dosing and/or higher input power. If the sawtooth activity is not maintained then central W accumulation is more likely to occur (Fig.12). Increasing core density may lead to suppression of W accumulation but at the expense of global confinement.

In L-mode plasmas the content of W decreases in the core while it increases to the outer target as the density increases and the temperature decreases. In this conditions, in spite the reduction of T_e in the divertor leading to a reduction of sputtering yields at the outer target, an increased W flux is observed which is explained by the transport of W from the core to the edge [36]. Application of core ICRH minority heating (up to 4MW) and/or more central NBI deposition have, also, been investigated with potentially encouraging results for W content control.

Normalised confinement in baseline H-modes tends to decrease with increasing gas fuelling levels. Similarly to JET-C data, the stationary discharges obtained in JET-ILW with large fuelling, and high density, exhibit confinement in the range $H_{98,y2}$~0.7-0.9. A major difference with respect to JET-C has been identified in high δ H-modes plasmas. Their confinement is significantly lower (20-30%) than equivalent JET-C cases and the access to a regime of good confinement at high gas fuelling has not yet been recovered with the JET-ILW.

The lower confinement observed in JET-ILW can be mainly attributed to lower edge pedestal temperatures. The trend is illustrated in Fig. 13 [37][38], where the temperature at the pedestal top (T_e-ped) normalised to the plasma current (I_p) is plotted versus the density at the pedestal top (n_e-ped) normalised to the Greenwald density (n_{gw}). A direct comparison of high δ pulses at 2.5MA, with the same power at the separatrix and the same density at the top of the pedestal, shows a reduction of the pedestal electron temperature by 30% (from ~1keV down to ~700eV) in the ILW case, while the profiles inside the pedestal show the same stiffness.

In addition, the type I ELMs in high deuterium fuelling pulses, at low pedestal temperatures,

exhibit a much slower crash of the edge electron temperature than similar JET-C cases and, consequently, a slower rise in divertor ELM heat load and reduced surface peak temperatures for a given drop in stored energy.

Experiments using nitrogen and neon seeding have been carried out in high and low δ plasmas. The most interesting results have been obtained in high-δ/2.5 MA plasmas (Fig.14) [39], where nitrogen seeding has been proven to raise both pedestal density and temperature with respect to un-seeded pulses. In these conditions the maximum confinement recovers to $H_{98,y2}$~0.92, close to equivalent nitrogen seeded pulses in JET-C. With nitrogen seeding the radiated power increases up to ~60% of the input power, cooling the edge plasma and reducing the inter-ELM W source, and the ELM frequency decreases. These plasmas, however, are still somewhat far from stationary conditions and tend to evolve towards behaviour dominated by W accumulation.

While it's obvious that the change in wall composition is at the root of the different baseline H-mode behaviour in ILW, the investigation of the specific effects causing W accumulation at low ELM frequency and low confinement in high δ configurations is progressing. Significant variations in core versus divertor radiation patterns, in impurity content and Z_{eff} as well as in neutral recycling have been identified and their impact on divertor, and core, plasma will be the subject of further analysis.

3.3 HYBRID H-MODE SCENARIO

The hybrid H-mode scenario offers the prospect of extended pulse length and H_{98}>1 at reduced plasma current with respect to the baseline H-mode.

Very promising results were obtained in JET-C and re-development of this scenario in JET-ILW has been an important area of research. The Hybrid H-mode scenario has been re-established in JET-ILW both at low and high triangularity at medium current values, up to 2MA and input power up to 24.1MW (as in Pulse No: 83328; NBI 23.4MW) [35]. As with the baseline H-modes, the operation range is somewhat restricted by W accumulation in discharges with no gas puffing. The amount of gas fuelling needed to control the W accumulation is, however, less than in comparable baseline plasmas. The pulse shown in Fig.15, with H_{98}~1.2 and β_N~2.8, is well within the typical scatter of results with the carbon wall (best pulses had H_{98}~1.4).

The pedestal pressure is lower in the high delta hybrid plasmas for JET-ILW compared to JET-C and the core profiles are more peaked, resulting in a similar overall confinement [38]. At low δ, similar global confinement to C-wall reference cases is obtained but with higher density and lower temperature. As in AUG with the W wall, optimisation of the central heating has been employed to avoid W core accumulation.

3.4 ELM MITIGATION

JET is equipped with several external methods to control the ELM activity and first experiments have been performed.

The JET High Frequency Pellet Injector (HFPI) [40] was implemented with the major goal to establish ELM pacing in ITER relevant scenarios with negligible fuelling. The particle flux rate for

ELM pacing at 50 Hz is expected to be about 1×10^{22} D/s corresponding to a rather low gas plasma fuelling rate. The Low Field Side (LFS) injection of 'pacing size' pellets, with about 1/3 of them arriving almost intact to the plasma although with a small scatter in size, has achieved a pacing efficiency up to 60%, resulting in an ELM frequency increase from 7 up to 31Hz. Pellets launched from the Vertical High Field Side (VHFS) showed low delivery efficiency from the injection system but significantly higher ELM trigger potential. Fuelling size pellets were injected reliably at 15Hz with a nominal pellet size of 22×10^{20} D; persistent ELM control was demonstrated in baseline H-mode discharges both with low and high triangularity.

The JET Error Field Correction Coils (EFCC), used to produce RMPs for ELM mitigation studies, have been recently upgraded, doubling their coil current capability up to 96kAt. This enhancement expanded the applicability of RMP as an ELM control/ suppression mechanism in plasmas with ITER-relevant materials in addition to the results obtained in other devices with different PFCs [41,42,43]. ELM mitigation experiments with magnetic perturbations have been performed at low and high collisionality in JET-ILW [44].

In the low collisionality JET-ILW plasmas (Fig.16) the use of EFCC for application of n = 2 field has the effect to increase the ELM frequency from 20Hz up to 80Hz. In addition, a reduction of ELM peak heat load due to multiple splitting of the outer strike point has been observed [44]. This was not observed in the previous JET-C EFCC ELM control experiments, at lower EFCC current. The amount of splitting seems to be linked to the amplitude of the perturbation field and the edge safety factor, q_{95}.

Strong mitigation of type-I ELMs was observed when a n = 2 field is applied at high collisionality ($\nu^*_e = 2.0$). Type-I ELMs ($f_{ELM} \sim 45$Hz) were replaced by high frequency small ELMs ($f_{ELM} \sim$ few hundreds Hz).

There is no drop in the core electron density and temperature during the application of the n = 2 field, even with EFCC time integrated current up to 88 kAt. Again, splitting of the outer strike point has been observed during the mitigation of the type-I ELMs. This experimental observation is similar to that observed with an n = 2 field in the high collisionality H-mode plasmas on AUG [42] with a full W wall. In contrast, the impact of the EFCC of an n = 2 field in high collisionality H-mode plasmas in JET-C was almost absent [45].

In addition to pellet pacing and EFCC, ELMs can be controlled at JET by rapid variations of the Radial Field, the so-called Vertical Kicks. This technique was already applied in JET-C H-mode plasmas, demonstrating that ELMs can be synchronised with the imposed kick frequency [46]. In JET-ILW only a limited number of kick experiments has been carried out so far, mostly under cold pedestal conditions typical of the high fuelling ILW H-modes. The preliminary indications are that full control of the ELM frequency can be obtained up to the maximum value explored of ~42Hz for radial field perturbations sligthly higher than in JET-C. Scans of both kick amplitude, from 3 to 12kV, and duration, from 1.5 to 4.5ms, have been carried out to investigate the physics of ELM triggering by kicks. Initial analysis suggests that the probability to trigger an ELM depends more strongly on the duration than on the amplitude of the kick.

CONCLUSIONS AND PERSPECTIVES

The first year of operation with the JET ILW has provided a number of important elements in view of the use of beryllium and tungsten as plasma facing materials in ITER. The expectation of low tritium retention has been confirmed, with a retention rate of 10^{20}D/s, in line with the ITER needs for an acceptable tritium inventory. Operation with beryllium and tungsten are characterized by reduced level of radiation and good ITER relevant break-down conditions (<0.35 Vm^{-1}). The reduction of radiated power leads to an increase of the thermal loads on PFCs during disruptions and to larger vessel forces. However, the use of massive gas injection has proven to mitigate JET disruptions efficiently up to high plasma current (3.5 MA) and it is now routinely used. The development of plasma scenarios has achieved important milestones, with the re-establishment of robust type-I ELMy H-mode and hybrid regimes with confinement 30% above the ITER scaling. High power type-I ELMy H-modes avoid tungsten accumulation due to lower W penetration at increased ELM frequencies (> 15 Hz). Pedestal characteristics tends to be different between the ILW and the carbon wall, with lower pedestal temperatures in the present configuration. Nitrogen seeding has been investigated, and has let to increased pedestal temperature similar to AUG.

The ILW exploitation will continue in 2013 with the main aim of demonstrating satisfactory operation in the presence of shallow melting of tungsten, in view of the final ITER decision on the use of tungsten. The progressive increase of plasma performance is the objective of the 2014 and 2015 campaigns. On the longer term, the preparation of a DT experiment is ongoing.

Following the completion of the feasibility studies for new JET enhancements, the design and R&D activity for a set of internal Resonant Magnetic Perturbation coils is being progressed in collaboration with the Institute for Plasma Research in Gandhinagar with the goal of being ready for a decision on the procurement of the full system by mid 2013.

ACKNOWLEDGMENTS

This work was supported by EURATOM and carried out within the framework of the European Fusion Development Agreement. The views and opinions expressed herein do not necessarily reflect those of the European Commission.

REFERENCES

[1]. R. Pitts, et al. Journal of Nuclear Materials,Volume **415**, Issue 1, p. S957-S964.
[2]. J. Pamela, et al. Journal of Nuclear Materials **363-365**, 1 – 11 (2007).
[3]. G.F. Matthews *et al.,* 2009 Physica Scripta **T138** 014030.
[4]. A. Kallenbach et al. Nuclear Fusion **49** (2009) 045007
[5]. S. Brezinsek et al., 24th IAEA Fusion Energy Conference (FEC2012), San Diego
[6]. R. Neu et al., Nuclear Fusion **45** (2005) 209
[7]. J.W. Coenen et al., 24th IAEA Fusion Energy Conference (FEC2012), San Diego
[8]. J. Roth et al., Plasma Physics and Controlled Fusion **50** (2008) 103001
[9]. M.H.R. Mayoral et al., 24th IAEA Fusion Energy Conference (FEC2012), San Diego

[10]. T. Putterich et al., 2008 Plasma Physics and Controlled Fusion **50** 085016
[11]. A. Czarnecka et al., 39th EPS Conference & 16th Int. Congress on Plasma Physics P5.047 (2012).
[12]. G van Rooij et al., 24th IAEA Fusion Energy Conference (FEC2012), San Diego
[13]. J.W. Coenen et al., 24th IAEA Fusion Energy Conference (FEC2012), San Diego
[14]. P.C. DeVries et al., 24th IAEA Fusion Energy Conference (FEC2012), San Diego
[15]. P.C. DeVries et al., 39th European Physical Society Conf. on Plasma Physics (EPS2012), Stockholm
[16]. H.T. Kim et al., 20th Int. Conf. on Plasma Surface Interactions in Controlled Fusion (Aachen, 2012)
[17]. J. Mailloux et al., 39th European Physical Society Conf. on Plasma Physics (EPS2012), Stockholm
[18]. J. Roth et al., Journal of Nuclear Materials **390-391**, 1–9 (2009)
[19]. T. Loarer et al., 20th Int. Con. on Plasma Surface Interactions in Controlled Fusion (Aachen, 2012)
[20]. V. Philipps et al., 20th Int. Conf. on Plasma Surface Interactions in Controlled Fusion (Aachen, 2012)
[21]. A. Huber et al., 20th Int. Conf. on Plasma Surface Interactions in Controlled Fusion (Aachen, 2012)
[22]. M. Groth et al., 24th IAEA Fusion Energy Conference (FEC2012), San Diego
[23]. V. Riccardo et al., 2004 Plasma Physics and Controlled Fusion **46** 925
[24]. C. Reux et al., 27th Symposium on Fusion Technology (SOFT-2012), Liege
[25]. V. Riccardo et al., 27th Symposium on Fusion Technology (SOFT-2012), Liege
[26]. I.M. Nunes et al., 24th IAEA Fusion Energy Conference (FEC2012), San Diego
[27]. G Arnoux et al., High Temperature Plasma Diagnostics (HTPD) 2012, Monterey, California
[28]. Ph .Mertens et al., 20th Int. Conf.on Plasma Surface Interactions in Controlled Fusion (Aachen, 2012)
[29]. Y.R. Martin et al., 2008 Journal of Physics: Conference Series **123** 012033
[30]. C.F. Maggi et al., 38th EPS Conference on Plasma Physics, (Strasbourg 2011)
[31]. Y. Andrew et al., Plasma Physics and Controlled Fusion **48** (2006) 479
[32]. C.F. Maggi et al., 39th European Physical Society Conf. on Plasma Physics (EPS2012), Stockholm
[33]. R. Neu et al., 20th Int. Conf. on Plasma Surface Interactions in Controlled Fusion (Aachen, 2012)
[34]. W. Fundamenski et al., Nuclear Fusion **52** (2012) 062003
[35]. E. Joffrin et al., 24th IAEA Fusion Energy Conference (FEC2012), San Diego
[36]. S. Brezinsek et al., 39th European Physical Society Conf.on Plasma Physics (EPS2012), Stockholm
[37]. L. Frassineti et al., 39th European Physical Society Conf. on Plasma Physics (EPS2012), Stockholm

[38]. MNA Beurskens et al., 24th IAEA Fusion Energy Conference (FEC2012), San Diego
[39]. C Giroud et al., 24th IAEA Fusion Energy Conference (FEC2012), San Diego
[40]. P Lang et al., Pedestal and Edge Physics ITPA meeting , Hefei, China
[41]. T Even et al., et al. Nature Physics **2**, 419 (2006)
[42]. Y Liang et al., Physical Review Letters **98**, 265004 (2007)
[43]. W. Suttrop, et al. Physical Review Letters **106**, 225004 (2011)
[44]. Y Liang et al., 24th IAEA Fusion Energy Conference (FEC2012), San Diego
[45]. Y Liang et al., Nuclear Fusion **50** 025013 (2010)
[46]. E de la Luna et al., 23rd IAEA Fusion Energy Conference, Daejon (2010)

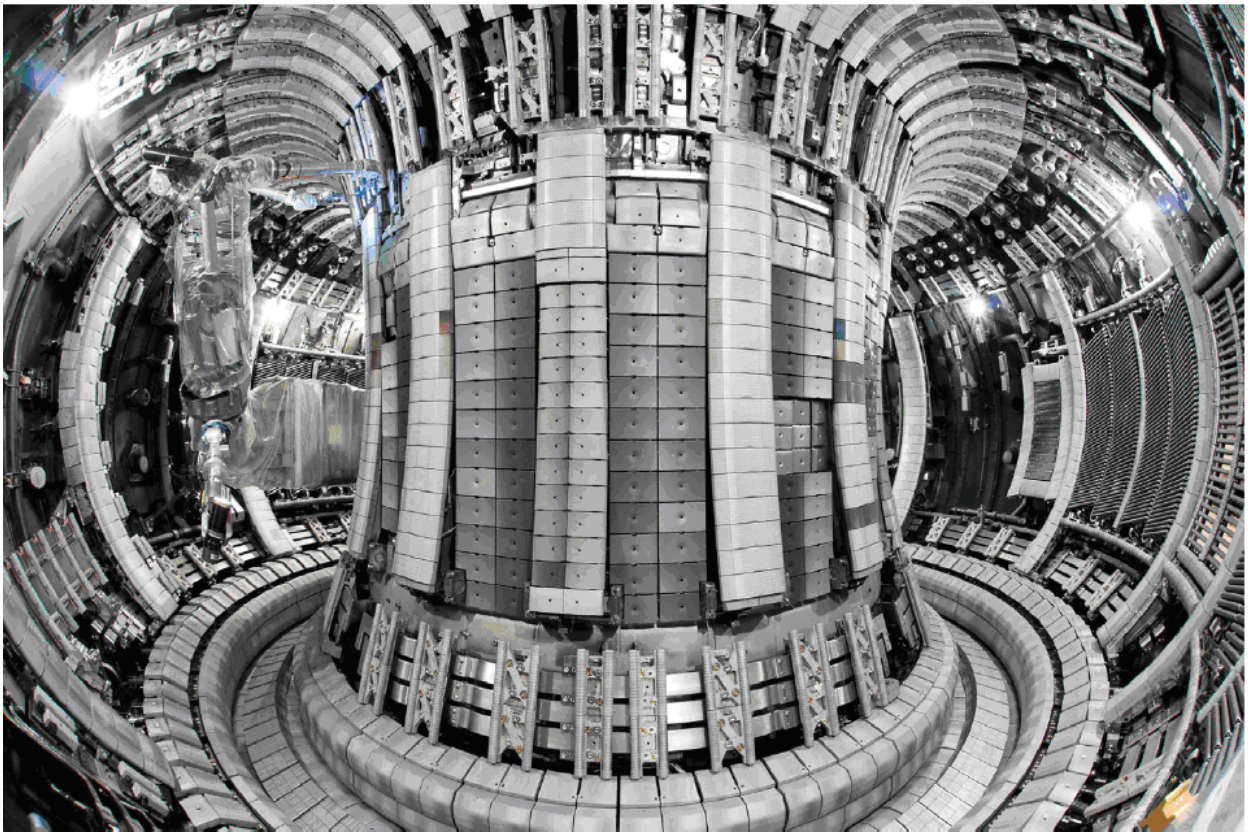

Figure 1: The new JET ITER-like wall. The main wall tiles are either bulk-Be or Be coated Inconel with W-coated tiles used for the NBI shine through areas and restraint rings.. The divertor is composed of bulk W tiles for the horizontal target and W-coated CFC tiles for the rest.

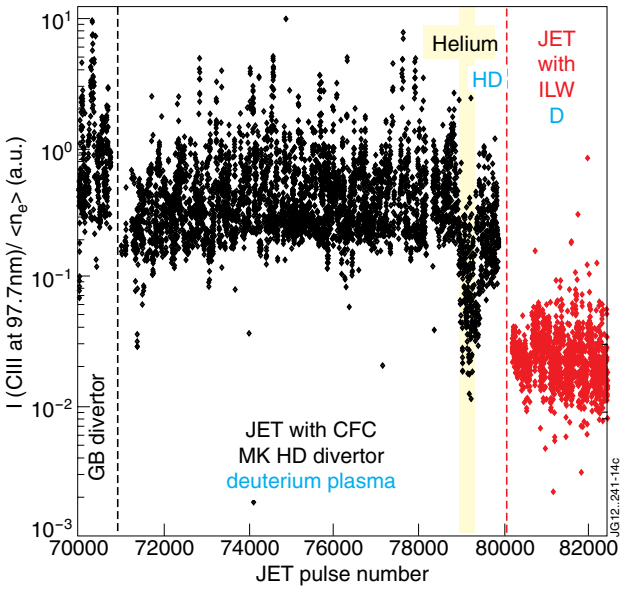

Figure 2: Evolution of the normalised carbon edge emission showing a clear decrease (~20×) after the installation of the ILW.

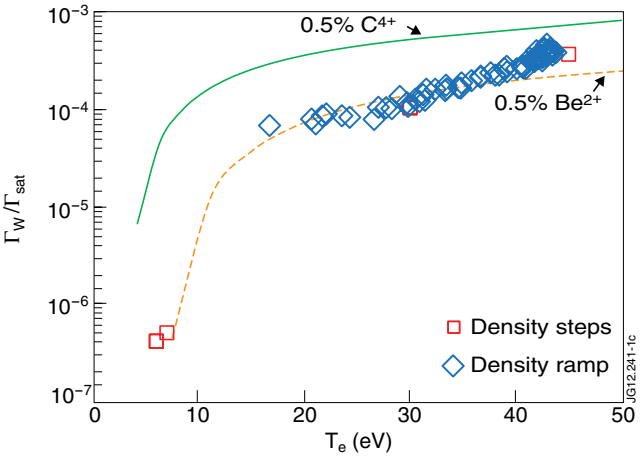

Figure 3: Effective W erosion yields measured in low power L-mode. Values follow very close the predicted erosion rates for a 0.5% (experimental) abundance of $Be2^+$. For comparison, the expected erosion yield for the impact of $C4^+$ ions is shown as green line.

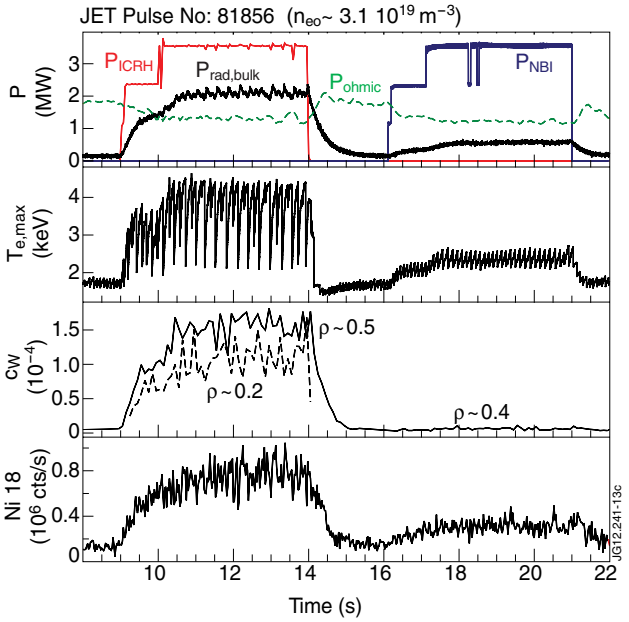

Figure 4: The effect of ICRF and neutral beam heating on plasma radiation, central elctron temperature, W conscentration and Ni emission in an L-mode plasma at constant density.

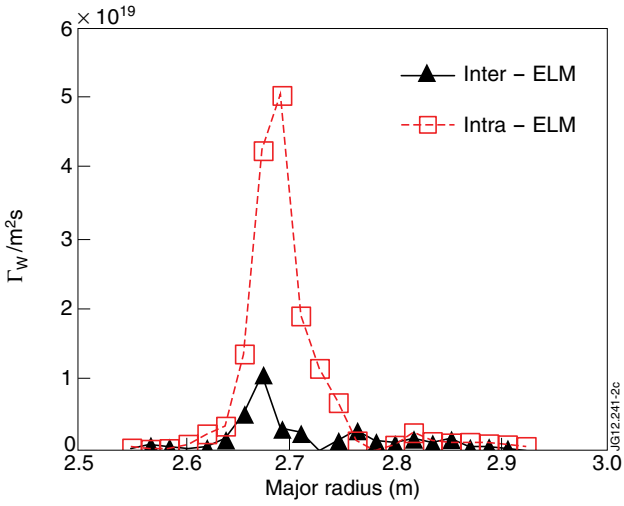

Figure 5: Comparison of the tungsten influx (time averaged) between and during ELMs. The graph shows clearly that intra-ELM W-sputtering is largely dominant (13 MW NBI, 7.5×10^{19} m^{-3} line averaged ne, 10Hz fELM).

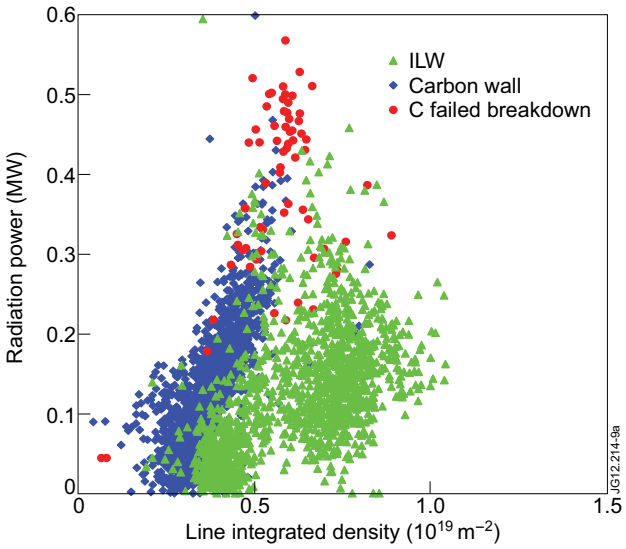

Figure 6: Radiation power versus line-integrated density at the end of the burn-through phase in JET.

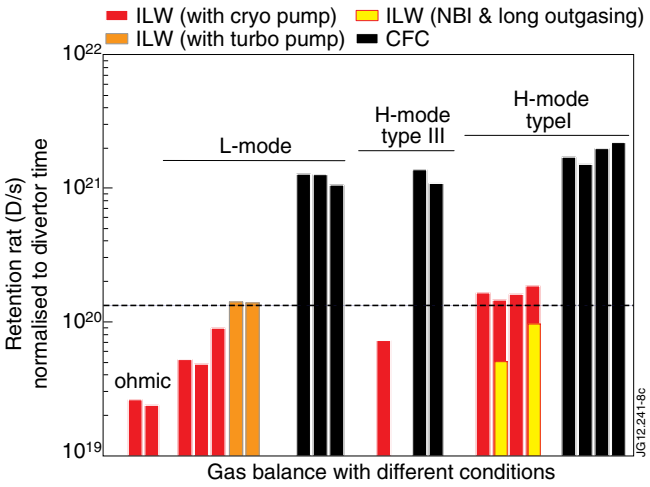

Figure 7: Retention rates for ILW and C wall in different types of plasma.

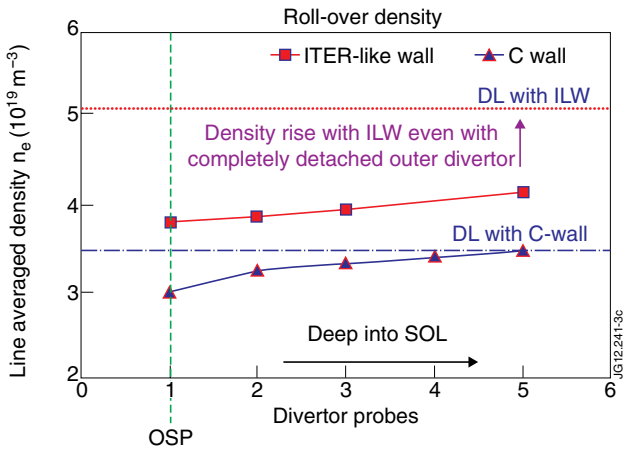

Figure 8: Roll-Over and density limits for operation with detached divertor for C machine and ILW. The density is measured by a Langmuir probe array along the divertor. In the ILW the detachment occurs at much lower density, below the L-H transition limit, giving larger margin for stable detachment operation.

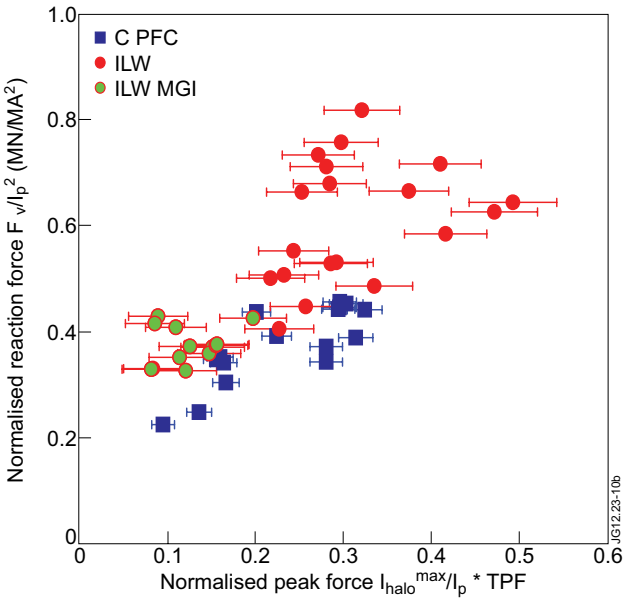

Figure 9: The equivalent static force required for the measured vessel excursion normalised to the plasma current squared versus the normalised halo current force for a set of high triangularity JET-C and JET-ILW disruptions. The green dots represent disruptions in JET-ILW with the use of MGI.

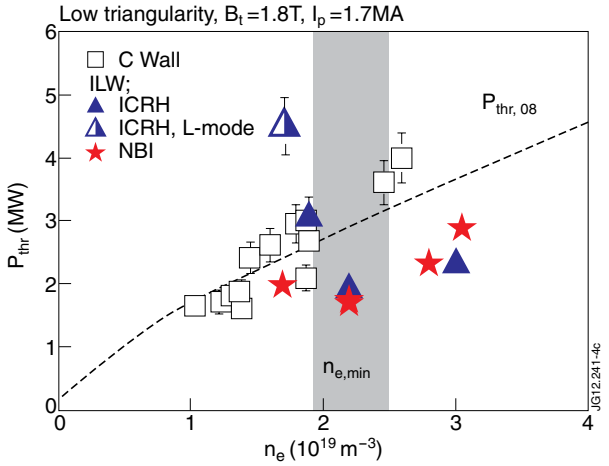

Figure 10: H-mode power threshold comparison between JET-C and JET-ILW.

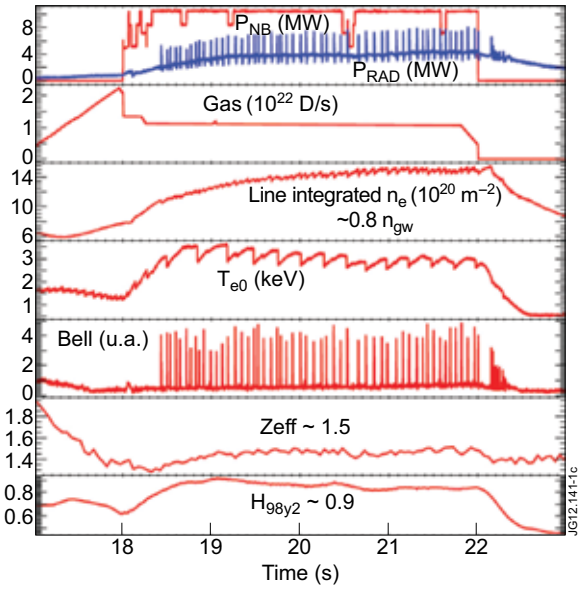

Figure 11: H_{98}~0.9 stationary discharge type I ELM baseline scenario with the JET ILW (NBI: 11MW).

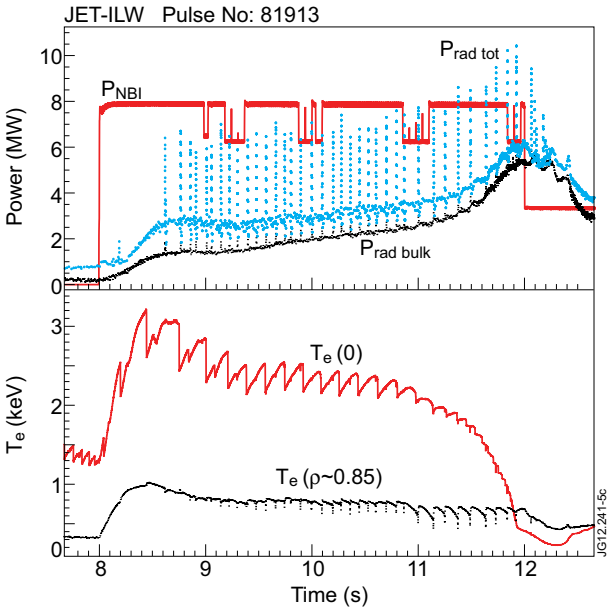

Figure 12: Extreme example of W peaking and accumulation. A rise in central radiated power leads to a collapse of the central temperature.

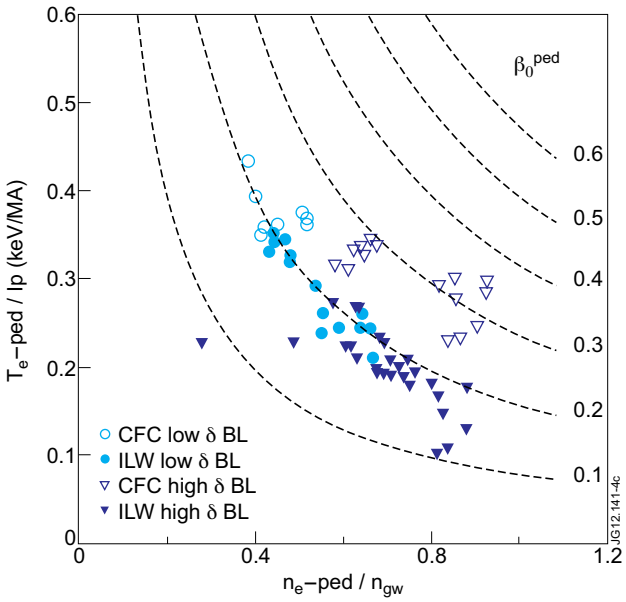

Figure 13: {$T_{e\text{-}ped}$/Ip, $n_{e\text{-}ped}$/ngw} diagram comparing C wall and ILW at 2.5MA/2.7T. (BL – baseline).

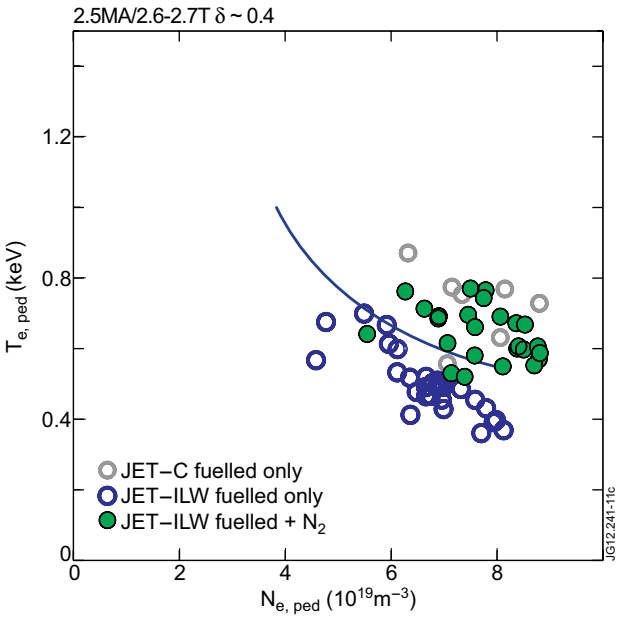

Figure 14: Pedestal n_e, T_e diagram for high triangularity pulses with similar input power (14-17MW). The data shows that JET-C pedestal conditions can be recovered in the JET-ILW via N_2 seeding.

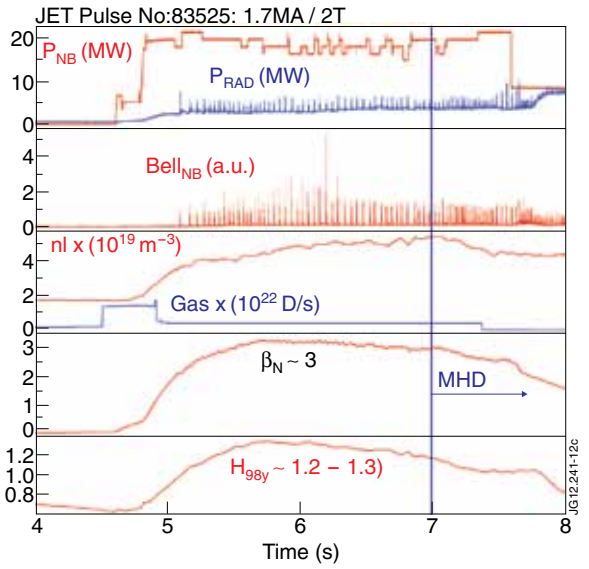

Figure 15: Example for a "hybrid" plasma (1.5MA / 2.0T) [35] in JET-ILW at $H_{98y2} > 1$ at low total radiated power and Z_{eff}.

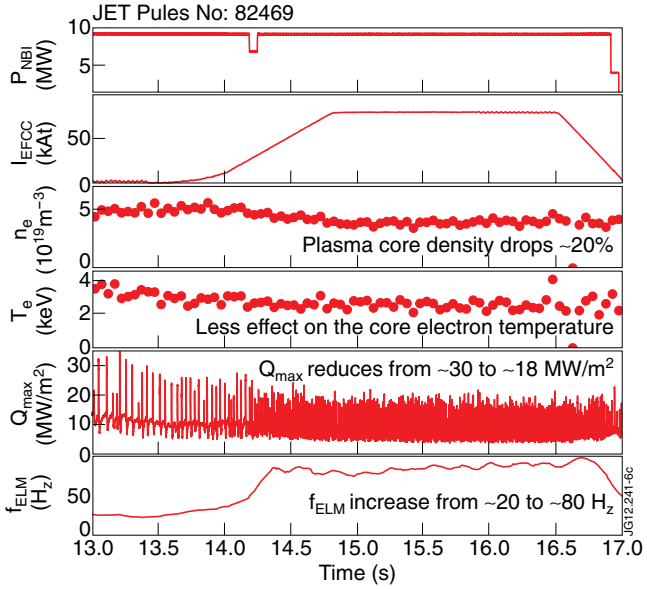

Figure 16: An example of ELM mitigation with the n = 2 field in a low collisionality type-I ELM H-mode plasma.

Appendix: List of JET EFDA Contributors

I. Abel[1], V. Afanesyev[2], M. Aftanas[3], G. Agarici[4], K.M. Aggarwal[5], L. Aho-Mantila[6], E. Ahonen[7], M. Aints[8], M. Airila[6], R. Akers[9], Th. Alarcon[4], R. Albanese[10], A. Alexeev[11,12], A. Alfier[13], P. Allan[9], S. Almaviva[14], A. Alonso[15], B. Alper[9], H. Altmann[9], D. Alves[16], G. Ambrosino[10], V. Amosov[12], F. Andersson[17], E. Andersson Sundén[18], V. Andreev[11], Y. Andrew[9], M. Angelone[19], M. Anghel[20], A. Anghel[21], C. Angioni[22], G. Apruzzese[19], N. Arcis[9], P. Arena[23], A. Argouarch[4], M. Ariola[10], A. Armitano[4], R. Armstrong[24], G. Arnoux[9], S. Arshad[25], G. Artaserse[10], J.F. Artaud[4], A. Ash[9], E. Asp[18], O. Asunta[7], C.V. Atanasiu[21], G. Atkins[9], L. Avotina[26], M.D. Axton[9], C. Ayres[9], A. Baciero[15], V. Bailescu[27], B. Baiocchi[28], R.A. Baker[9], I. Balboa[9], M. Balden[22], C. Balorin[4], N. Balshaw[9], J.W. Banks[9], Y.F. Baranov[9], D. Barbier[4], I.L. Barlow[9], M.A. Barnard[9], R. Barnsley[5], L. Barrena[15], L. Barrera[15], M. Baruzzo[13], V. Basiuk[4], G. Bateman[29], P. Batistoni[19], N. Baumgarten[30], L. Baylor[31], B. Bazylev[32], P.S. Beaumont[9], K. Beausang[24], M. Bécoulet[4], N. Bekris[33,32], M. Beldishevski[9], A.C. Bell[9], F. Belli[19], M. Bellinger[9], T. Bellizio[10], P.S.A. Belo[16], É. Belonohy[22], P.E. Bennett[9], N.A. Benterman[9], G. Berger-By[4], H. Bergsåker[34], H. Berk[35], J. Bernardo[16], M. Bernert[22], B. Bertrand[4], M.N.A. Beurskens[9], B. Bieg[36], B. Bienkowska[36], T.M. Biewer[31], M. Bigi[13], P. Bílková[3], W. Bin[28], J. Bird[9], J. Bizarro[16], C. Björkas[37], T.R. Blackman[9], P. Blanchard[38], E. Blanco[15], J. Blum[39], V. Bobkov[22], A. Boboc[9], D. Boilson[24], I. Bolshakova[40], T. Bolzonella[13], L. Boncagni[19], G. Bonheure[41], X. Bonnin[4], D. Borba[33,16], A. Borthwick[9], A. Botrugno[19], C. Boulbe[39], F. Bouquey[4], C. Bourdelle[4], K.v. Bovert[30], M. Bowden[9], T. Boyce[9], H.J. Boyer[9], A. Bozhenkov[30], R.J. Brade[9], J.M.A. Bradshaw[9], J. Braet[42], V. Braic[43], G.C. Braithwaite[9], C. Brault[4], B. Breizman[35], S. Bremond[4], P.D. Brennan[9], A. Brett[9], J. Breue[44], S. Brezinsek[30], M.D.J. Bright[9], F. Briscoe[9], M. Brix[9], M. Brombin[13], B.C. Brown[9], D.P.D. Brown[9], J. Brzozowski[34], J. Bucalossi[4], M.A. Buckley[9], T. Budd[9], R.V. Budny[45], P. Bunting[9], P. Buratti[19], G. Burcea[27], A. Burckhart[22], P.R. Butcher[9], R.J. Buttery[46], P. Cahyna[3], G. Calabrò[19], C.P. Callaghan[9], J.P. Caminade[4], P.G. Camp[9], D.C. Campling[9], R. Caniello[28], J. Canik[31], B. Cannas[47], A.J. Capel[9], G. Carannante[10], P.J. Card[9], A. Cardinali[19], T. Carlstrom[46], P. Carman[9], D. Carralero[15], L. Carraro[13], T. Carter[48], B.B. Carvalho[16], I. Carvalho[16], P. Carvalho[16], A. Casati[4], C. Castaldo[19], J. Caughman[31], R. Cavazzana[13], M. Cavinato[13], M. Cecconello[18], E. Cecil[45], F.E. Cecil[49], A. Cenedese[13], C. Centioli[19], R. Cesario[19], C.D. Challis[9], M. Chandler[9], C. Chang[50], A. Chankin[22], I.T. Chapman[9], B. Chektybayev[51], M. Chernyshova[36], D.J. Child[9], P. Chiru[21], G. Chitarin[13], I. Chugonov[2], I. Chugunov[2], D. Ciric[9], F. Clairet[4], R.H. Clarke[9], R. Clay[9], M. Clever[30], J.P. Coad[9,6], P.A. Coates[9], V. Cocilovo[19], S. Coda[38], R. Coelho[16], J. Coenen[30], I. Coffey[5], L. Colas[4], M. Cole[31], S. Collins[9], S. Combs[31], J. Compan[44], J.E. Conboy[9], S. Conroy[18], N. Cook[9], S.P. Cook[9], D. Coombs[9], S.R. Cooper[9], Y. Corre[4], G. Corrigan[9], S. Cortes[16], D. Coster[22], G.F. Counsell[9], X. Courtois[4], M. Cox[9], T. Craciunescu[21], S. Cramp[9], F. Crisanti[19], G. Croci[28], O. Croft[9], K. Crombe[52], K. Crombé[53], B.J. Crowley[9], N. Cruz[16], G. Cseh[54], L. Cupido[16], M. Curuia[20], R.A. Cusack[9], A. Czarnecka[36], T. Czarski[36], S. Dalley[9], E.T. Daly[9], A. Dalziel[9], R. Daniel[55], D. Darrow[45], O. David[56], N. Davies[9], W. Davies[45], J.J. Davis[9], I.E. Day[9], C. Day[32], R. De Angelis[19], G. de Arcas[57], M.R. de Baar[58], E. de la Cal[15], E. de la Luna[15,33], J.L. de Pablos[15], G. De Tommasi[10], P.C. de Vries[58], R. De-Angelis[19], F. Degli Agostini[13], E. Delabie[58], D. del-Castillo-Negrete[31], L. Delpech[4], G. Denisov[59],

A.J. Denyer[9], R.F. Denyer[9], S. Devaux[22], P. Devynck[4], L. Di Matteo[19], L. Di Pace[19], P.J. Dirken[9], T. Dittmar[60], A. Dnestrovskiy[11], D. Dodt[22], R. Doerner[60], S. Doldatov[52], K. Dominiczak[44], P. Dooley[33,19], S.E. Dorling[9], D. Douai[4], A.P. Down[9], P.T. Doyle[9], J.R. Drake[34], T. Dreischuh[61], V. Drozdov[9], P. Dumortier[53], D. Dunai[54], I. Duran[3], F. Durodié[53], P. Dutta[55], R. Dux[22], K. Dylst[42], R. Eaton[9], T. Edlington[9], A.M. Edwards[9], D.T. Edwards[9], P.K. Edwards[9], Th. Eich[22], A. Ekedahl[4], T. Elevant[34], B. Ellingboe[24], C.G. Elsmore[9], B. Emmoth[62], G. Erdei[63], G. Ericsson[18], L.G. Eriksson[64], A. Eriksson[17], B. Esposito[19], H.G. Esser[30], T. Estrada[15], E.A. Evangelidis[65], G.E. Evans[9], G.D. Ewart[9], D.T. Ewers[9], G. Falchetto[4], D. Falie[21], J.G.A. Fanthome[9], J.W. Farthing[9], A. Fasoli[38], B. Faugeras[39], N. Fedorczak[4], R.C. Felton[9], C. Fenzi[4], A. Fernades[16], H. Fernandes[16], J.A. Ferreira[15], J. Ferreira[16], J. Ferron[46], J.A. Fessey[9], L. Figini[28], J. Figueiredo[33], A. Figueiredo[16], J. Figueiredo[16], P. Finburg[9], K.H. Finken[30], U. Fischer[32], N. Fitzgerald[24], J. Flanagan[9], C. Fleming[9], A.D. Forbes[9], O. Ford[1], A. Formisano[10], D. Fraboulet[4], R.J. Francis[9], L. Frassinetti[34], R. Fresa[10], J.P. Friconneau[56], D. Frigione[19], K. Fullard[9], W. Fundamenski[9], M. Furno Palumbo[10], K. Gál[54], X. Gao[66], S. Garavaglia[28], X. Garbet[4], J. Garcia[4], M. Garcia Munoz[22], W. Gardner[31], P. Garibaldi[4], D. Garnier[4], L. Garzotti[9], M. Gatu Johnson[18], P. Gaudio[14], E. Gauthier[4], J.W. Gaze[9], D.F. Gear[9], J. Gedney[9], S.J. Gee[9], M. Gelfusa[14], E. Genangeli[33,19], S. Gerasimov[9], A. Geraud[4], T. Gerbaud[4,58], M. Gherendi[21], N. Ghirelli[4], J.C. Giacalone[4], L. Giacomelli[41], C.S. Gibson[9], C. Gil[4], S.J. Gilligan[9], C.G. Gimblett[9], D. Gin[2], E. Giovannozzi[19], C. Giroud[9], G. Giruzzi[4], J. Godwin[9], J.K. Goff[9], P. Gohil[46], A. Gójska[36], V. Goloborod'ko[67], B. Gonçalves[16], M. Goniche[4], S. Gonzales[15], S.M. González de Vicente[42], A. Goodyear[9], N. Gorelenkov[45], G. Gorini[41], R. Goulding[31], B. Graham[9], D. Graham[9], M.E. Graham[9], J. Graves[38], N.R. Green[9], H. Greuner[22], E. Grigore[21], F.S. Griph[9], C. Grisolia[4], G. Gros[4], M. Groth[7], S. Grünhagen[9], M.P. Gryaznevich[9], R. Guirlet[4], J. Gunn[4], A. Gupta[30], P. Guzdar[68], L.J. Hackett[9], S. Hacquin[4], B. Haist[9], A. Hakola[6], M. Halitovs[26], S.J. Hall[9], S.P. Hallworth Cook[9], D.T. Hamilton[9], H. Han[69], R.C. Handley[9], S. Harding[9], J.D.W. Harling[9], D. Harting[30], M.J. Harvey[9], T.D.V. Haupt[9], N.C. Hawkes[9], R. Hawryluk[45], J.H. Hay[9], N. Hayashi[50], P.W. Haydon[9], I.R. Hayward[9], S. Hazel[9], P.J.L. Heesterman[9], W. Heidbrink[45], K. Heinola[37], C. Hellesen[18], T. Hellsten[34], O.N. Hemming[9], T.C. Hender[9], M. Henderson[70], V. Hennion[4], C. Hidalgo[15], S. Higashijima[50], J.W. Hill[9], M. Hill[9], K. Hill[45], J. Hillairet[4], D. Hillis[31], T. Hirai[44], M. Hitchin[9], J. Hobirk[22], C. Hogan[31], C.H.A. Hogben[9], G.M.D. Hogeweij[58], I.C. Hollingham[9], R. Holyaka[40], D.A. Homfray[9], G. Honeyands[9], S.H. Hong[4], J.H. Hong[71], J. Horácek[3], B.A. Horn[9], A.R. Horton[9], L.D. Horton[33,64], S.P. Hotchin[9], M.R. Hough[9], W. Houlberg[31], D.F. Howell[9], A. Huber[30], T.M. Huddleston[9], Z. Hudson[9], M. Hughes[9], M. Hühnerbein[44], C.C. Hume[9], A.J. Hunt[9], C.L. Hunter[9], T.S. Hutchinson[9], S. Huygen[53], G. Huysmans[4], S. Ide[50], C. Illescas[15], F. Imbeaux[4], D. Ivanova[34], I. Ivanova-Stanik[36], E. Ivings[9], S. Jachmich[53], G. Jackson[46], P. Jacquet[9], K. Jakubowska[36], P.V. James[9], F. Janky[3], A. Järvinen[7], S. Jednorog[36], I. Jenkins[9], M.A.C. Jennison[9], C. Jeskins[9], O. Jin Kwon[72], E. Joffrin[4,33], M.F. Johnson[9], R. Johnson[9], T. Johnson[34], D. Jolovic[30], V. Jonauskas[73], E.M. Jones[9], G. Jones[9], H.D. Jones[9], T.T.C. Jones[9], M. Jouvet[4], C. Jupén[74], I. Kachtchouk[12], J. Kaczmarczyk[36], A. Kallenbach[22], J. Källne[75], D. Kalupin[30], S. Kálvin[54], G. Kamelander[76], R. Kamendje[77], K. Kamiya[50], A. Kappatou[78], W. Kasparek[79], G. Kasprowicz[36], I. Katramados[9], G. Kaveney[9], A.S. Kaye[9], M.J. Kear[9], D.L. Keeling[9], D. Kelliher[24],

M. Kempenaars[9], P. Khilar[9], E. Khilkevich[2], N.G. Kidd[9], M. Kiisk[8], K.M. Kim[69], H. Kim[69], R.F. King[9], D.J. Kinna[9], V. Kiptily[9], G. Kirnev[11], N. Kirneva[11], K. Kirov[9], A. Kirschner[30], R. Kisielius[73], D. Kislov[11], G. Kiss[30], G. Kizane[26], A. Klein[80], C. Klepper[31], N. Klimov[12], A. Klix[32], M. Knaup[30], K. Kneuper[9], H. Kneupner[30], P.J. Knight[9], S.J. Knipe[9], M. Kocan[4], R. Koch[53], F. Köchl[76], G. Kocsis[54], S. Koivuranta[6], T. Koppitz[44], A. Korotkov[9], T. Koskela[7], H.R. Koslowski[30], V. Kotov[30], M.D. Kovari[9], G. Kramer[45], A. Krasilnikov[12], V. Krasilnikov[12], S. Kraus[30], A. Kreter[30], K. Krieger[22], A. Kritz[29], Y. Krivchenkov[9], U. Kruezi[30], S. Krylov[11], I. Ksiazek[36], S. Kuhn[67], W. Kühnlein[44], A. Kukushkin[11], A. Kundu[55], T. Kurki-Suonio[7], A. Kurowski[36], B. Kuteev[11], A. Kuyanov[11], V. Kyrytsya[53], R. La Haye[46], M. Laan[8], C. Labate[10], A. Lachichi[9], L. Laguardia[28], N. Lam[9], P. Lang[22], M.T. Large[9], A. Lasa[37], I. Lassiwe[30], J.R. Last[9], K.D. Lawson[9], M. Laxåback[34], R.A. Layne[9], F. Le Guern[4], B. LeBlanc[45], S. Lee[81], J. Lee[69], H.J. Leggate[24], M. Lehnen[30], M. Leigheb[19], I. Lengar[82], M. Lennholm[33,64], E. Lerche[53], C.N. Lescure[9], Y. Li[80], A. Li Puma[4], Y. Liang[30], J. Likonen[6], Y. Lin[80], V. Lindholm[7], J. Linke[44], S.A. Linstead[9], B. Lipshultz[80], X. Litaudon[4], A.G. Litvak[59], Y. Liu[9,66], T. Loarer[4], A. Loarte[70], R.C. Lobel[9], P.J. Lomas[9], F.D. Long[9], J. Lönnroth[7], D.J. Looker[9], J. Lopez[15], Ph. Lotte[4], F. Louche[53], M.J. Loughlin[9], A.B. Loving[9], C. Lowry[33,64], T. Luce[46], R.M.A. Lucock[9], A. Lukanitsa[83], A. Lukin[84], A.M. Lungu[21], C.P. Lungu[21], A. Lyssoivan[53], P. Macheta[9], A.S. Mackenzie[9], M. Macrae[9], G. Maddaluno[19], G.P. Maddison[9], J. Madsen[85], B. Magesh[55], P. Maget[4], C.F. Maggi[22], H. Maier[22], J. Mailloux[9], T. Makkonen[7], M. Makowski[46], A. Malaquias[33,16], C.J. Manning[9], M. Mansfield[24], M.E. Manso[16], P. Mantica[28], N. Marcenko[12], M.A. Marchitti[10], M. Mardenfeld[45], J.L. Marechal[4], M. Marinelli[14], M. Marinucci[19], D. Marocco[19], C.A. Marren[9], S. Marsen[86], D. Martin[9], D.L. Martin[9], G. Martin[4], Y. Martin[38], J.R. Martín-Solís[87], K. Masaki[50], A. Masiello[13], C. Maszl[67], S. Matejcik[88], A. Matilal[9], M. Mattei[10], G.F. Matthews[9], S. Mattoo[55], D. Matveev[52], F. Maviglia[10], C.R. May[9], M. Mayer[22], M.L. Mayoral[9], D. Mazon[4], C. Mazzotta[19], E. Mazzucato[45], P. McCarthy[24], K.G. McClements[9], K. McCormick[22], P.A. McCullen[9], D. McCune[45], D.C. McDonald[9], R. Mcgregor[9], J.P. Mckivitt[9], A. Meakins[9], F. Medina[15], A.G. Meigs[9], M. Menard[46], L. Meneses[16], S. Menmuir[89], I.R. Merrigan[9], Ph. Mertens[30], A. Messiaen[53], B. Mészáros[54], H. Meyer[9], G. Miano[10], R. Michling[32], M. Miele[10], J. Miettunen[7], P. Migliucci[14], A.G. Miller[9], S.F. Mills[9], J.J. Milnes[9], K. Min Kim[69], T. Mindham[9], E. Miorin[28], F. Mirizzi[19], E. Mirones[15], M. Mironov[2], R. Mitteau[4], J. Mlynár[3], P. Mollard[4], I. Monakhov[9], P. Monier-Garbet[4], R. Mooney[9], D. Moreau[4], Ph. Moreau[4], L. Moreira[9], A. Morgan[9], P.D. Morgan[9], C. Morlock[90,30], A.W. Morris[9], G.L. Mort[9], M. Murakami[31], A. Murari[33,13], I. Mustata[21], F. Nabais[16], T. Nakano[50], E. Nardon[4], G. Nash[9], V. Naulin[85], M.F.F. Nave[16], R. Nazikian[45], I. Nedzelski[16], C.R. Negus[9], J.D. Neilson[9], G. Nemtsev[12], A. Neto[16], R. Neu[22], O. Neubauer[30], G.J. Newbert[9], M. Newman[9], K.J. Nicholls[9], A. Nicolai[30], L. Nicolas[4], P. Nieckchen[90,22], A.H. Nielsen[85], S.K. Nielsen[85], P. Nielsen[13], G. Nielson[45], J. Nieto[57], M.P.S. Nightingale[9], D. Nishijima[55], C. Noble[9], M. Nocente[41], H. Nordman[17], M. Norman[9], S. Nowak[28], I. Nunes[16], M. Oberkofler[22], M. Odstrcil[3], T. O'Gorman[24], T. Ohsako[50], M. Okabayashi[45], S. Olariu[91], A. Oleynikov[12], M. O'Mullane[92], J. Ongena[53], F. Orsitto[19], O.I. Oswuigwe[9], M. Ottaviani[4], N. Oyama[50], D. Pacella[19], K. Paget[9], E. Pajuste[26], S. Palazzo[23], J. Palénic[88], J. Pamela[4], S. Pamela[4], L. Pangione[9], A. Panin[30], S. Panja[55], A. Pankin[29], A. Pantea[21], V. Parail[9], P. Paris[8], Th.

Parisot[4], M. Park[81], A. Parkin[9], A. Parsloe[9], B.T. Parsons[9], R. Pasqualotto[13], P. Pastor[4], R. Paterson[9], M.K. Paul[30], D. Peach[9], R.J.H. Pearce[9], B.J. Pearson[9], I.J. Pearson[9], L.C. Pedrick[9], M.A. Pedrosa[15], B. Pegourie[4], R. Pereira[16], P. Pereslavtsev[32], A. Perevezentsev[9], Ch. Perez von Thun[33,22], V. Pericoli-Ridolfini[90,19], A. Perona[93], Y. Perrot[56], S. Peruzzo[13], S. Peschanyy[32], G. Petravich[54], L. Petrizzi[19], V. Petrov[12], V. Petrzilka[3], V. Philipps[30], F. Piccolo[9], A. Pietropaolo[28], M. Pillon[19], S.D. Pinches[9], T. Pinna[19], G. Pintsuk[44], P. Piovesan[13], A. Pironti[10], F. Pisano[47], R. Pitts[70], B. Plaum[79], V. Plyusnin[16], M. Polasik[36], F.M. Poli[94], N. Pomaro[13], O. Pompilian[21], L. Poncet[4], P.J. Pool[9], S. Popovichev[9], F. Porcelli[93], M.T. Porfiri[19], C. Portafaix[4], A. Pospieszczyk[30], G. Possnert[75], K. Pozniak[36], S. Pradhan[55], R. Pragash[55], V. Prajapati [55], G. Prestopino[14], P. Prior[9], R. Prokopowicz[36], M.E. Puiatti[13], K. Purahoo[9], V. Pustovitov[11], Th. Pütterich[22], D. Püttmann-Kneupner[30], A. Quercia[10], E. Rachlew[89], R. Rademaker[33], T. Rafiq[29], M.S.J. Rainford[9], G. Ramogida[19], J. Rapp[30], J.J. Rasmussen[85], K. Rathod[55], G. Rattá[15], G. Ravera[19], D. Refy[54,63], R. Reichle[4], M. Reinelt[22], D. Reiser[30], R. Reiss[4], D. Reiter[30], D. Rendell[9], C. Reux[4], G. Rewoldt[80], T.T. Ribeiro[16], V. Riccardo[9], D. Richards[9], F. Rigollet[4], F.G. Rimini[64], L. Rios[15], M. Riva[19], J.E.C. Roberts[9], R.J. Robins[9], D.S. Robinson[9], S.A. Robinson[9], D.W. Robson[9], H. Roche[4], M. Rödig[44], N. Rodionov[12], V. Rohde[22], A. Rolfe[9], M. Romanelli[9], F. Romanelli[33,19], A. Romano[19], J. Romero[15], E. Ronchi[18], S. Rosanvallon[4], Ch. Roux[4], S. Rowe[9], M. Rubel[34], G. Rubinacci[10], M. Ruiz[57], C. Ruset[21], M. Russell[9], A. Ruth[24], L. Ryc[36], A. Rydzy[19], J. Rzadkiewicz[36], S. Saarelma[9], F. Sabathier[4], R. Sabot[4], S. Sadakov[30], A. Sadvakassova[51], A. Sadykov[51], P. Sagar[9], G. Saibene[25], A. Saille[4], F. Saint-Laurent[4], M. Salewski[85], A. Salmi[6], F. Salzedas[16], U. Samm[30], P. Sanchez[15], S. Sanders[9], S.G. Sanders[9], G. Sandford[9], K. Sandland[9], P. Sandquist[17], D.E.G. Sands[9], M.I.K. Santala[7], P. Santra[55], F. Sartori[25], R. Sartori[25], O. Sauter[38], A. Savelyev[2], A. Savtchkov[30], S.C. Scales[9], A. Scarabosio[22], N. Schaefer[4], V. Schmidt[13], A. Schmidt[30], O. Schmitz[30], S. Schmuck[86], M. Schneider[4], M. Scholz[36], K. Schöpf[67], B. Schweer[30], J. Schweinzer[22], M. Seki[50], L. Semeraro[19], A. Semerok[95], G. Sergienko[30], M. Sertoli[22], M.M.J. Shannon[9], S.E. Sharapov[9], S.R. Shaw[9], A. Shevelev[2], B. Sieglin[22], R. Sievering[44], C.A. Silva[16], P.A. Simmons[9], A. Simonetto[28], D. Simpson[9], S.K. Sipilä[7], A.C.C. Sips[33,64], P. Sirén[6], A. Sirinelli[9], H. Sjöstrand[18], D. Skopintsev[12], K. Slabkowska[36], P.G. Smith[9], J. Snipes[80], L. Snoj[82], S. Snyder[29], S. Soare[20], E.R. Solano[15], A. Soleto[15], W. Solomon[45], C. Soltane[4,33], P. Sonato[13], A. Sopplesa[13], A. Sorrentino[10], J. Sousa[16], C.B.C. Sowden[9], C. Sozzi[28], P. Späh[32], T. Spelzini[9], J. Spence[9], F. Spineanu[21], P. Spuig[4], R.D. Stagg[9], M.F. Stamp[9], V. Stancalie[21], P. Stangeby[46], R. Stankiewicz[36], C. Stan-Sion[91], D.E. Starkey[9], M.J. Stead[9], M. Stejner[85], A.V. Stephen[9], M. Stephen[55], A.L. Stevens[9], R.B. Stokes[9], D. Stork[9], D. Stoyanov[61], J. Strachan[45], P. Strand[17], M. Stransky[17], D. Strauss[32], D. Strintzi[78], W. Studholme[9], Y. Su Na[69], F. Subba[93], H.P. Summers[92], Y. Sun[30], C. Surdu-Bob[21], E. Surrey[9], D.J. Sutton[9], J. Svensson[86], D. Swain[31], B.D. Syme[9], I.D. Symonds[9], T. Szabolics[54], T. Szepesi[54], A. Szydlowski[36], F. Tabares[15], V. Takalo[96], H. Takenaga[50], T. Tala[6], A.R. Talbot[9], C. Taliercio[13], C. Tame[9], M. Tardocchi[28], L. Taroni[13], G. Telesca[52], A. Terra[30], A.O. Terrington[9], D. Testa[38], J.M. Theis[4], J.D. Thomas[9], P.D. Thomas[9], P.R. Thomas[25], V.K. Thompson[9], C. Thomser[30], A. Thyagaraja[9], P.A. Tigwell[9], I. Tiseanu[21], R. Tivey[33,64], J.M. Todd[9], T.N. Todd[9], M.Z. Tokar[30], S. Tosti[19], P. Trabuc[4], J.M. Travere[4], P. Trimble[9], A. Trkov[82], E. Trukhina[11], M. Tsalas[58,65], E. Tsitrone[4], D. Tskhakaya

jun[67], O. Tudisco[19], S. Tugarinov[12], M.M. Turner[24], S.G.J. Tyrrell[9], N. Umeda[50], B. Unterberg[30], H. Urano[50], A.J. Urquhart[9], I. Uytdenhouwen[42], A. Vaccaro[32], A.P. Vadgama[9], G. Vagliasindi[19], D. Valcarcel[16], M. Valisa[13], J. Vallory[4], M. Valovic[9], D. Van Eester[53], B. van Milligen[15], G.J. van Rooij[58], C.A.F. Varandas[16], S. Vartanian[4], K. Vasava[55], V. Vdovin[11], J. Vega[15], G. Verdoolaege[52], J.M. Verger[4], L. Vermare[4], C. Verona[14], Th. Versloot[58], M. Vervier[53], J. Vicente[16], S. Villari[19], E. Villedieu[4], F. Villone[10], J.E. Vince[9], G.J. Vine[9], I. Vinyar[84], B. Viola[10], E. Vitale[19], R. Vitelli[14], A. Vitins[26], M. Vlad[21], I. Voitsekhovitch[9], M. Vrancken[53], K. Vulliez[4], C.W.F. Waldon[9], M. Walker[9], M.J. Walsh[9], J. Waterhouse[9], M.L. Watkins[9,33], M.J. Watson[9], T. Wauters[4,53], M.W. Way[9], C.R. Webb[9], J. Weiland[17], H. Weisen[38,33], M. Weiszflog[18], R. Wenninger[22], A.T. West[9], J.M. Weulersse[95], M.R. Wheatley[9], A.D. Whiteford[92], A.M. Whitehead[9], A.G. Whitehurst[9], A.M. Widdowson[9], C. Wiegmann[30], S. Wiesen[30], A. Wilson[9], D. Wilson[9], D.J. Wilson[9], H.R. Wilson[97], M. Wischmeier[22], D.M. Witts[9], R.C. Wolf[30], J. Wolowski[36], P. Woscov[80], J. Wright[80], G.S. Xu[66], V. Yavorskij[67], V. Yerashok[40], M. Yoo[69], J. Yorkshades[9], C. Young[9], D. Young[9], I.D. Young[9], X. Yuhong[53], S. Yun[81], L. Zabeo[9], W. Zabolotny[36], L. Zaccarian[19], R. Zagorski[90,36], F.S. Zaitsev[88,83], L. Zakharov[45], R. Zanino[93], V. Zaroschi[21], K.D. Zastrow[9], I. Zatz[45], B. Zefran[82], W. Zeidner[22], M. Zerbini[19], T. Zhang[30], A. Zhitlukin[12], Y. Zhu[66], O. Zimmermann[30], V. Zoita[33,21], S. Zoletnik[54], W. Zwingman[4],

[1] Imperial College, University of London, London, SW7 2AZ, UK

[2] Ioffe Physico-Technical Institute, 26 Politekhnicheskaya, St Petersburg 194021, Russian Federation

[3] Association EURATOM-IPP.CR, Institute of Plasma Physics AS CR, Za Slovankou 3, 182 21 Praha 8, Czech Republic

[4] Association EURATOM-CEA, CEA/DSM/IRFM, Cadarache 13108 Saint Paul Lez Durance, France

[5] Department of Pure and Applied Physics, Queens University, Belfast, BT7 1NN, UK

[6] VTT Technical Research Centre of Finland, Association EURATOM-Tekes, P.O.Box 1000, FIN-02044 VTT, Finland

[7] Aalto University, Association EURATOM-Tekes, P.O.Box 14100, FIN-00076 Aalto, Finland

[8] University of Tartu, Ülikooli 18, 50090 Tartu, Estonia

[9] Euratom/CCFE Fusion Association, Culham Science Centre, Abingdon, Oxon, OX14 3DB, UK

[10] Associazione EURATOM-ENEA sulla Fusione, Consorzio CREATE, Via Claudio 21, 80125 Napoli, Italy

[11] NRC Kurchatov Institute, 1 Kurchatov Square, Moscow 123182, Russian Federation

[12] Troitsk Insitute of Innovating and Thermonuclear Research (TRINITI), Troitsk 142190, Moscow Region, Russian Federation

[13] Associazione EURATOM-ENEA sulla Fusione, Consorzio RFX Padova, Italy

[14] Associazione EURATOM-ENEA sulla Fusione, Università di Roma, Italy

[15] Laboratorio Nacional de Fusion, Asociacion EURATOM-CIEMAT, Madrid, Spain
[16] Associação EURATOM/IST, Instituto de Plasmas e Fusão Nuclear, Instituto Superior Técnico, Av Rovisco Pais, 1049-001 Lisbon, Portugal
[17] Association EURATOM-VR, Department of Earth and Space Sciences, Chalmers University of Technology, SE-41296 Gothenburg, Sweden
[18] Association EURATOM-VR, Department of Physics and Astronomy, Uppsala University, SE-75120 Uppsala, Sweden
[19] Associazione EURATOM-ENEA sulla Fusione, C.R. Frascati, Roma, Italy
[20] The National Institute for Cryogenics and Isotopic Technology, Association EURATOM-MEdC, Ramnicu Valcea, Romania
[21] The National Institute for Laser, Plasma and Radiation Physics, Association EURATOM-MEdC, Magurele-Bucharest, Romania
[22] Max-Planck-Institut für Plasmaphysik, EURATOM-Assoziation, D-85748 Garching, Germany
[23] Dipartimento di Ingegneria Elettrica Elettronica e dei Sistemi-Università degli Studi di Catania, 95125 Catania, Italy
[24] Dublin City University (DCU), Ireland
[25] Fusion for Energy Joint Undertaking, Josep Pl. 2, Torres Diagonal Litoral B3, 08019, Barcelona, Spain
[26] University of Latvia, 19 Raina Blvd., Riga, LV 1586, Latvia
[27] The Nuclear Fuel Plant, Pitesti, Romania
[28] IFP-CNR, EURATOM-ENEA-CNR Association on Fusion, via R. Cozzi 53, 20125 Milano, Italy
[29] Lehigh University, Bethlehem, PA 18015, Pennsylvania, USA
[30] Forschungszentrum Jülich, Institute of Energy Research - Plasma Physics, EURATOM Association, D-52425, Jülich, Germany
[31] Oak Ridge National Laboratory, Oak Ridge, TN 37831-6169, Tennessee, USA
[32] Karlsruhe Institute of Technology, P.O.Box 3640, D-76021 Karlsruhe, Germany
[33] EFDA Close Support Unit, Culham Science Centre, Culham, OX14 3DB, UK
[34] Association EURATOM-VR, Fusion Plasma Physics, EES, KTH, SE-10044 Stockholm, Sweden
[35] University of Texas at Austin, Institute for Fusion Studies, Austin, TX 78712, Texas, USA
[36] Association Euratom-IPPLM, Hery 23, 01-497 Warsaw, Poland
[37] University of Helsinki, Association EURATOM-Tekes, P.O. Box 43, FI-00014 University of Helsinki, Finland
[38] Association EURATOM-Confédération Suisse, Ecole Polytechnique Fédérale de Lausanne (EPFL), CRPP, CH-1015 Lausanne, Switzerland
[39] Laboratoire J.A.Dieudonné, Université de Nice-Sophia-Antipolis, Parc Valrose, F-06108 Nice CEDEX 02, France

[40] Magnetic Sensor Laboratory (LPNU), 1 Kotliarevsky Str, Lviv, 79013, Ukraine
[41] University Milano-Bicocca, EURATOM-ENEA-CNR Association on Fusion, piazza della Scienza 3, 20126 Milano, Italy
[42] Association EURATOM-SCK-CEN, Nuclear Research Centre, 2400 Mol, Belgium
[43] The National Institute for Optoelectronics, Magurele-Bucharest, Romania, Association EURATOM-MEdC
[44] Forschungszentrum Jülich, Institute of Energy Research, EURATOM Association, D-52425, Jülich, Germany
[45] Princeton Plasma Physics Laboratory, James Forrestal Campus, Princeton, NJ 08543, New Jersey, USA
[46] General Atomics, P.O.Box 85608, San Diego, CA 92186-5608, California, USA

[47] Department of Electrical and Electronic Engineering, University of Cagliari, Piazza d'Armi 09123 Cagliari, Italy
[48] University of California, 1111 Franklin St., Oakland, CA 94607, USA
[49] Colorado School of Mines, 1500 Illinois Street, Golden, CO 80401, Colorado, USA
[50] Japan Atomic Energy Agency, Naka Fusion Research Establishment, Nakamachi, Naka-gun, Ibaraki-ken 311-0913, Japan
[51] ASE Institute of Atomic Energy, RSE NNC RK, Krasnoarmeyskaya 10, Kurchatov, V-Kazakhstanskaya, Kazakhstan
[52] Department of Applied Physics UG (Ghent University) St-Pietersnieuwstraat 41 B-9000 Ghent Belgium
[53] Association "EURATOM - Belgian State" Laboratory for Plasma Physics Koninklijke Militaire School - Ecole Royale Militaire Renaissancelaan 30 Avenue de la Renaissance B-1000 Brussels Belgium
[54] Association EURATOM/HAS, Wigner Research Centre for Physics, P.O.B. 49, H - 1525 BUDAPEST
[55] Institute for Plasma Research, Bhat, Gandhinagar - 382 428, Gujarat State, India
[56] CEA/Fontenay aux Roses, B.P.6 F-92265 Fontenay-aux-roses CEDEX, France
[57] Universidad Politécnica de Madrid, Grupo I2A2, Madrid, Spain
[58] FOM Institute DIFFER P.O. Box 1207 NL-3430 BE Nieuwegein, The Netherlands
[59] Institute of Applied Physics, Nizhny Novgorod 603155, Russian Federation
[60] University of California, San Diego, 9500 Gilman drive, La Jolla, CA 92093, United States
[61] Association EURATOM-INRNE Institute of Elecronics, Bulgarian Academy of Sciences, 72 Tzarigradsko shosse, Sofia 1784, Bulgaria
[62] Association EURATOM-VR, Department of Material Physics, ICT, KTH, SE-16440 Kista, Sweden
[63] Association EURATOM-HAS, Budapest Univeristy of Technology and Economics, H-1111 Budapest, Hungary

[64] European Commission, B-1049 Brussels, Belgium
[65] Association EURATOM-Hellenic Republic, NCSR “Demokritos” 153 10, Agia Paraskevi Attikis, Greece
[66] Institute of Plasma Physics, Chinese Academy of Sciences, Hefei, 230031, China
[67] University of Innsbruck, Association EURATOM-Österreichische Akademie der Wissenschaften (ÖAW), Austria
[68] Institute for Plasma Research, University of Maryland, College Park, MD 20742-3511, Maryland, USA
[69] Seoul National University, Shilim-Dong, Gwanak-Gu, Republic of Korea
[70] ITER Organization, Route de Vinon, CS 90 046, 13067 Saint Paul Lez Durance, France
[71] 291 Daehak-ro(373-1 Guseong-dong), Yuseong-gu, Daejeon 305-701, Republic of Korea
[72] Daegu University, Jillyang, Gyeongsan, Gyeongbuk 712-174, Republic of Korea
[73] Association EURATOM-LEI, Breslaujos str. 3, LT-44403, Kaunas, Lithuania
[74] Association EURATOM-VR, Department of Physics, Lund University, SE-22100 Lund, Sweden
[75] Association EURATOM-VR, Department of Engineering Sciences, Uppsala University, SE-75120 Uppsala, Sweden
[76] Vienna University of Technology, Association EURATOM-Österreichische Akademie der Wissenschaften (ÖAW), Austria
[77] Physics Section, Division of Physical and Chemical Sciences, International Atomic Energy Agency, P.O. Box 100, Wagramer Strasse 5, A-1400 Vienna, Austria
[78] Association EURATOM-Hellenic Republic, National Technical University of Athens, Iroon Politechniou 9, 157 73 Zografou, Athens, Greece
[79] IPF, Stuttgart University, Stuttgart, Germany
[80] MIT Plasma Science and Fusion Centre, Cambridge, MA 02139, Massachusetts, USA
[81] Gwahangno 169-148 (Eoeun-dong), Yusung-gu, Daejeon, Korea 305-806
[82] Association EURATOM-MHST, Jozef Stefan Institute, Reactor Physics Department, Jamova 39, SI-1000 Ljubljana, Slovenia
[83] Moscow State University, Moscow 119991, Russian Federation
[84] 27a, Gzhatskaya Ulitsa, Saint Petersburg, 195220, Russia
[85] Association EURATOM-DTU, Technical University of Denmark, Department of Physics, DTU Risø Campus, P.O.Box 49, DK-4000 Roskilde, Denmark
[86] Max-Planck-Institut für Plasmaphysik, Teilinsitut Greifswald, EURATOM-Assoziation, D-17491 Greifswald, Germany
[87] Departamento de Física, Universidad Carlos III de Madrid, 28911 Leganés, Madrid, Spain
[88] Department of Experimental Physics, Faculty of Mathematics, Physics and Informatics Comenius University Mlynska dolina F2, 84248 Bratislava, Slovak Republic
[89] Association EURATOM-VR, Department of Physics, SCI, KTH, SE-10691 Stockholm, Sweden

[90] EFDA Close Support Unit, D-85748 Garching, Germany
[91] The “Horia Hulubei” National Institute for Physics and Nuclear Engineering, Association EURATOM-MEdC, Magurele-Bucharest, Romania
[92] Department of Physics and Applied Physics, University of Strathclyde, Glasgow, G4 ONG, UK
[93] Associazione EURATOM-ENEA sulla Fusione, Politecnico di Torino, Italy
[94] Department of Physics, University of Warwick, Coventry, CV4 7AL, UK
[95] CEA/Saclay, F-91191 Gif-sur-Yvette CEDEX, France
[96] Tampere University of Technology, Association EURATOM-Tekes, P.O. Box 527, FI-33101 Tampere, Finland
[97] University of York, Heslington, York YO10 5DD, UK